HHS Public Access

Author manuscript

Dev Dyn. Author manuscript; available in PMC 2019 February 01.

Published in final edited form as:

Dev Dyn. 2018 February ; 247(2): 304–314. doi:10.1002/dvdy.24605.

Pten regulates neural crest proliferation and differentiation during mouse craniofacial development

Tianfang Yang, **Matthew Moore**, and **Fenglei He***

Department of Cell and Molecular Biology, Tulane University, New Orleans, LA 70118, USA

Abstract

Background—The Phosphatase and tensin homolog deleted on chromosome TEN (*Pten*) is implicated in a broad range of developmental events and diseases. However, its role in neural crest and craniofacial development has not been well illustrated.

Results—Using genetically engineered mouse models, we showed that inactivating *Pten* specifically in neural crest cells causes malformation of craniofacial structures. *Pten* conditional knockout mice exhibit perinatal lethality with overgrowth of craniofacial structures. At cellular level, *Pten* deficiency increases cell proliferation rate and enhances osteoblast differentiation. Our data further revealed that inactivating *Pten* elevates PI3K/AKT signaling activity in neural crest derivatives, and confirmed that attenuation of PI3K/AKT activity led to decreased neural crest cell proliferation and differentiation both *in vitro* and *in vivo*.

Conclusions—Our study revealed that *Pten* is essential for craniofacial morphogenesis in mice. Inactivating *Pten* in neural crest cells increases proliferation rate and promotes their differentiation towards osteoblasts. Our data further indicate that Pten acts via modulating PI3K/AKT activity during these processes.

Keywords

Pten; PI3K/Akt; neural crest cells; proliferation; differentiation

Introduction

Neural crest cells (NCCs) are a unique cell population and play an important role during vertebrate development. They are originated as ectodermal cells at the border of neural plate at the dorsal neural tube and transform into mesenchymal cells by epithelial-mesenchymal transformation (EMT). Subsequently, NCCs migrate extensively from the dorsal region to the ventral destinations, where they differentiate into a broad range of cell types and contribute to organogenesis (Selleck and Bronner-Fraser, 1995).

Craniofacial morphogenesis is a highly orchestrated process and is dependent on NCCs (Chai and Maxson, 2006). Lineage studies reveal that cranial NCCs contribute predominantly to the craniofacial mesenchyme (Chai et al., 2000; Jiang et al., 2000; Yoshida et al., 2008). During craniofacial development, NCCs give rise to cartilage, bone, glial cells,

*Corresponding author: Telephone: (504) 865-5059, fhe@tulane.edu.

peripheral neurons, pigment cells and connective tissues. NCC proliferation and differentiation are under rigorous regulation of a genetic network composed of multiple growth factors, receptors and their intracellular effectors (Knecht and Bronner-Fraser, 2002; Sauka-Spengler and Bronner-Fraser, 2008; Cordero et al., 2011).

The Phosphatase and Tensin homolog deleted on chromosome TEN (Pten) was discovered as a tumor suppressor as its mutation was frequently identified in human tumors (Li and Sun, 1997; Steck et al., 1997). Pten is a lipid phosphatase with a primary role in antagonizing the phosphatidylinositol-3-kinase (PI3K) signaling pathway, which is implicated in multiple processes including cell survival, proliferation, and differentiation (Steelman et al., 2004). Upon stimulation by growth factors, PI3K family members phosphorylate the second messenger phosphatidylinositol 4,5-bisphosphate (PIP_2) into phosphatidylinositol 3,4,5-trisphosphate (PIP_3), which activates downstream signaling cascades. Pten modulates PI3K signaling activity by converting PIP_3 to PIP_2 during this process. Besides its primary role of PI3K signaling inhibitor, Pten is also implicated in autophagy signaling of cancer cells (Arico et al., 2001; Errafiy et al., 2013).

Pten also plays a crucial role for embryonic development (Di Cristofano et al., 1998; Salmena et al., 2008). *Pten* null mutant mice die by E7.5, and heterozygotes develop phenotypes in the prostate, skin and colon, indicating an essential role for *Pten* in these tissues (Di Cristofano et al., 1998). In addition, accumulating evidence has demonstrated a role for *Pten* in development of retina, brain, neural stem cells and other tissues (Veleva-Rotse and Barnes, 2014). In the developing craniofacial tissues, previous studies showed that phosphorylated Pten is expressed in palate and tooth mesenchymal cells, as well as in oral and dental epithelial cells (Cho et al., 2008; Kero et al., 2016). However, the role of *Pten* in neural crest and craniofacial development still remains to be fully elucidated.

In the present study, we showed that *Pten* regulates neural crest development and craniofacial morphogenesis in mice. Interestingly, inactivating *Pten* in neural crest cells elevates Akt phosphorylation level in both trigeminal ganglia and craniofacial skeletons, but causes distinct phenotypes. In the trigeminal ganglia, inactivating *Pten* increases the rate of cellular proliferation, while in the premaxilla, *Pten* deficiency enhances both cell proliferation and osteoblast differentiation. On the other hand, inhibiting PI3K/AKT signaling activity in primary cells rescues *Pten* mutant phenotype. We further confirm these findings in Pdgfra PI3K signaling mutant mice. In summary, our study showed that *Pten* regulates neural crest proliferation and differentiation via modulating PI3K/AKT signaling pathway during mammalian craniofacial development.

Results

Pten is essential for mouse neural crest development and craniofacial morphogenesis

To investigate the role of *Pten* in neural crest development and craniofacial morphogenesis, we generated neural crest-specific *Pten* conditional knockout mice $Pten^{fl/fl}$; *Wnt1Cre2* by crossing $Pten^{fl/fl}$ (Groszer et al., 2001) with *Wnt1Cre2* transgenic line (Lewis et al., 2013). $Pten^{fl/fl}$; *Wnt1Cre2* mice exhibit 100% perinatal lethality with enlarged heads (Fig 1A–B; n=3). Morphometric analysis revealed that $Pten^{fl/fl}$; *Wnt1Cre2* embryo heads are comparable

to their littermate controls at E13.5 (Fig 1C, n=3). At E17.5, *Pten*$^{fl/fl}$; *Wnt1Cre2* embryo heads are 15±3% larger along the dorsal-ventral axis (a) and 34±5% larger along the anterior-posterior axis (b), while the length of their trunks is comparable to that of the control (data not shown, n=3). Skeletal preparations confirmed that *Pten*$^{fl/fl}$; *Wnt1Cre2* embryos exhibit an enlarged skull at E18.5 (Fig 1D–E, n=3). Morphometric analysis of the E18.5 skulls revealed that neural crest derived frontal bone of mutant embryos is 39±8% (n=6, $P<0.05$) larger that that of littermate controls, and mesoderm derived parietal bone of mutant embryos are 12±7% larger than controls (n=6, $p<0.05$). However, at E13.5, only mutant frontal bones are larger than the control (1.39±0.08 fold, n=6, $P<0.05$), while mutant parietal bones and the control show comparable length (1.08±0.02 fold, n=6, $P>0.05$). These results indicate that *Pten* plays an autonomous role in neural crest-derived frontal bone development, and the enlarged parietal bone at E18.5 is likely secondary to malformation of other structures.

To reveal the details of *Pten*$^{fl/fl}$; *Wnt1Cre2* craniofacial phenotype, we performed histological analysis on mutant embryos and littermate controls at E13.5 and E16.5. Hematoxylin/Eosin staining on frontal sections of E13.5 embryos showed that *Pten*$^{fl/fl}$; *Wnt1Cre2* and the control are comparable at the anterior level (Fig 2A, B). At the middle and posterior level, the midbrain of the mutant is larger than that of control (Fig 2C–F), consistent with previous studies that report *Pten* is important for brain development (Groszer et al., 2001; Marino et al., 2002; Yue et al., 2005; Fraser et al., 2008; Lehtinen et al., 2011). Interestingly, we observed that the trigeminal ganglion (tgg) is enlarged in the mutant (Fig 2E, F). At E16.5, the mutant premaxilla appears larger than the control (Fig 2G, H), and the regions of maxillary nerves (mn) and tgg are enlarged in the mutant embryos when compared to the littermate controls (Fig 2I–L).

Cranial neural crest cells give rise to the bones, cartilages, and neurons. To identify the cell types of mutant tissues showing abnormality, we conducted alkaline phosphatase-Alcian blue (AP-AB) staining on control and mutant embryos. Our results confirmed elevated AP activity in mutant premaxilla, frontal bones, mandible and palatine bones (Fig 3A–H), and the cartilage formation was not altered. Real time PCR results showed that osteoblast markers *Runx2* and *Sp7* exhibit comparable expression levels in the control and mutant, while expression level of *Osteocalcin* is significantly increased in the mutant embryos (Fig 3I). Increased *Osteocalcin* expression was further confirmed by section *in situ* hybridization in the mutant pmx at E15.5 (Fig 3J, K), suggesting that inactivating *Pten* promotes osteoblast maturation. Immunostaining for neurofilaments revealed increased neuronal formation in mutant mn and tgg at E13.5 (Fig. 3L–O). These results indicate that *Pten* controls osteogenesis and neuron formation during craniofacial morphogenesis.

Pten transcripts are expressed in craniofacial tissues in developing mouse embryos

Next we examined the expression pattern of *Pten* transcripts in the developing craniofacial tissues. *In situ* hybridization results revealed that *Pten* mRNA is expressed in the premaxilla and tgg of the control embryos (Fig. 4A, C). In *Pten*$^{fl/fl}$; *Wnt1Cre2* mice, *Pten* expression was efficiently deleted in both tissues (Fig 4B, D). These data indicated an autonomous role for *Pten* in regulating premaxilla and tgg development.

Inactivating *Pten* in neural crest cells increases cell proliferation rate of pmx osteoprogenitors and tgg

To understand the cellular mechanisms underlying *Pten*$^{fl/fl}$; *Wnt1Cre2* craniofacial phenotype, we assayed the cell proliferation rate, with a focus on the pmx osteoblasts and tgg neurons. BrdU labeling assay showed that at E13.5, 26±4% of pmx cells and 10±3% of tgg cells are proliferating in the control embryos; in the mutant, 57±8% of pmx cells and 21±6% of tgg cells are proliferating (Fig 5A–E, n=6, $P<0.05$). Further analysis showed that mutant pmx cells shows higher proliferation rate than control at E10.5 (1.3±0.1 fold), E12.5 (1.1±0.1 fold) and E15.5 (1.5±0.4 fold) (n=6, $P<0.05$). These results indicate that *Pten* controls cell proliferation rate in these neural crest derived tissues.

Inactivating *Pten* enhances AKT signaling activity in neural crest derivatives

To examine Pten downstream signaling pathways in neural crest development, we assayed both autophagy and PI3K/AKT signaling activity. Our data showed that expression of autophagy markers LC3-B and ubiquitin were not altered in mutant craniofacial structures (data not shown). Previous studies showed that in multiple cell types, Pten functions via antagonizing PI3K/AKT signaling pathway, which has been identified as an important player of craniofacial development (Fantauzzo and Soriano, 2015). Therefore, we examined if PI3K/AKT signaling activity is altered in *Pten*$^{fl/fl}$; *Wnt1Cre2* embryos. Immunohistochemistry results showed that expression of phosphorylated AKT is maintained at basal level in the control embryos, but is significantly increased in *Pten*$^{fl/fl}$; *Wnt1Cre2* pmx and tgg (Fig 6A, B, C and D). Western blot confirmed a 3.2±0.5 fold increase of phosphorylated AKT expression in the mutant pmx lysates (Fig 6E and F, n=3). Our data showed that *Pten* regulates the phosphorylation of AKT *in vivo* during craniofacial morphogenesis, and indicated that *Pten* might control NCC development via AKT signaling.

Inhibiting AKT signaling rescues *Pten* mutant cell proliferation and differentiation

To examine the role of AKT signaling in neural crest cells, we isolated the premaxilla tissues from E13.5 embryos and used them for primary cell culture. Western blot results showed that expression level of phosphorylated AKT of the mutant cells is significantly higher than the control (15.6±0.3 fold change), and treating mutant cells with AKT signaling inhibitor LY294002 (LY) decreases phosphorylated AKT expression (4.9±0.2 fold change relative to the mutant) (Fig 7A, B, H). BrdU labeling and AP staining showed that LY treatment inhibits cell proliferation rate (from 35±1% to 4%±1%) (Fig 7B–D, I; n=3) and AP activity (Fig 7E–G) of mutant cells. These results indicate that AKT signaling plays an important role in neural crest cell proliferation and differentiation, and Pten acts via AKT signaling to regulate neural crest cells.

Attenuation of PI3K signaling affects neural crest cell proliferation and osteogenesis *in vivo*

To examine if AKT mediates *Pten* regulation of neural crest development *in vivo*, we analyzed *Pdgfra*$^{PI3K/PI3K}$ embryos, in which the ability of Pdgfra to activate PI3K signaling is abrogated (Klinghoffer et al., 2002). BrdU labeling showed that cell proliferation rate of pmx oestoprogenitors is decreased in *Pdgfra*$^{PI3K/PI3K}$ embryos compared to the control

(57±18%) (Fig 8A, B and E, n=4, P<0.05). On the other hand, cell proliferation rate of tgg is not significantly altered in *Pdgfra*$^{PI3K/PI3K}$ mice (86±14%) (Fig 8C, D and E, n=6, P>0.05). AP activity in the pmx of *Pdgfra*$^{PI3K/PI3K}$ embryo at E13.5 is attenuated compared to the control (Fig 8F, F′, G, and G′). These results confirmed that PI3K signaling is critical to maintain neural crest cell proliferation and osteoblast differentiation *in vivo*.

Discussion

Originally discovered as a tumor suppressor gene, *Pten* is now recognized as an important player in development of multiple tissues. Previous studies assayed *Pten* expression in developing orafacial tissues (Cho et al., 2008; Kero et al., 2016), but it remains unclear if *Pten* is required for normal craniofacial morphogenesis. Our study showed that *Pten* plays critical roles in craniofacial development by regulating neural crest cell proliferation and differentiation. Our data also indicates that Pten might function via inhibiting PI3K/AKT signaling during mouse craniofacial development.

Pten is important for brain development. The brain overgrowth phenotype we found in *Pten*$^{fl/fl}$; *Wnt1Cre2* mice is consistent with previous reports in *Pten* conditional knockout using other *Cre* lines expressed in embryonic brains (Groszer et al., 2001; Marino et al., 2002; Yue et al., 2005; Fraser et al., 2008; Lehtinen et al., 2011). The craniofacial phenotype of *Pten*$^{fl/fl}$; *Wnt1Cre2* mice could thus be intrinsic, or secondary to the brain malformation, or combination of both. *In situ* hybridization showed that *Pten* transcripts are detected in the osteoprogenitors support the notion that *Pten* plays a primary role in these cells development (Fig 4). In addition, our data revealed that both cell proliferation and AKT phosphorylation were altered in the pmx bones of *Pten*$^{fl/fl}$; *Wnt1Cre2* embryos (Fig 5 and Fig 6). Although these findings cannot exclude the effect of brain overgrowth on craniofacial phenotype in the mutant, it highlights the autonomous role for *Pten* in neural crest and craniofacial development.

There are two pathways to form a bone. In long bones, the mesenchymal cells form a cartilaginous template for osteoblasts through endochondral ossification pathway. In calvarial and partial facial bones, osteoprogenitors differentiate into osteoblasts via the intramembranous pathway. *Pten* has been implicated in both these processes. During endochondral ossification, *Pten* was found to be essential for chondrocyte patterning and differentiation in the growth plate of long bones, as well as proliferation of osteoblast progenitors (Ford-Hutchinson et al., 2007; Yang et al., 2008; Hsieh et al., 2009; Guntur et al., 2011). In intramembranous ossification, inactivation of *Pten* using osteocalcin-*Cre* led to increased calvarial bone density (Zhang et al., 2002). Neural crest cells give rise to the entire facial skeleton. Our data showed that deletion of *Pten* in neural crest cells elevated proliferation rate and enhanced differentiation in osteoprogenitors of pmx (Fig 3 and Fig 5). However, we did not observe an obvious phenotype in the facial cartilages (Fig 3A–H).

Platelet derived growth factor receptors (PDGFRs) are major regulators of PI3K signaling in craniofacial development (Klinghoffer et al., 2002). *Pdgfra*$^{PI3K/PI3K}$ mice exhibit decreased proliferation of neural crest cells during craniofacial development (He and Soriano, 2013; Fantauzzo and Soriano, 2014; Fantauzzo and Soriano, 2015), and PDGFAA treatment

stimulates neural crest cell proliferation and differentiation via PI3K/AKT pathway (Vasudevan et al., 2015). All of the studies supported the notion that PI3K signaling is critical for craniofacial development. Our data showed that *Pten*$^{fl/fl}$; *Wnt1Cre2* mice exhibited a reversed phenotype to *Pdgfra*$^{PI3K/PI3K}$ in proliferation and differentiation of neural crest-derived osteoprogenitors (Fig 3, 5 and 8). These results confirmed the essential role for PI3K in craniofacial development. Interestingly, cell proliferation rate in *Pten*$^{fl/fl}$; *Wnt1Cre2* tgg is increased significantly but not affected in that of *Pdgfra*$^{PI3K/PI3K}$ mice. This result suggests that PDGFRa might play a dispensable role in the regulation of PI3K/AKT signaling and cell proliferation in tgg or Pten might act via other pathways to control tgg development.

Experimental Procedures

Animals

All animal experimentation was approved by the Institutional Animal Care and Use Committee of Tulane University. *Tg(Wnt1-cre)2Sor* (Lewis et al., 2013), referred to as *Wnt1Cre2; Pten*^{tm1Hwu} (Groszer et al., 2001), referred to as *Pten*$^{+/fl}$; and *Pdgfra*^{tm5Sor} (Klinghoffer et al., 2002), referred to as *PDGFRα*$^{+/PI3K}$, were maintained on a C57BL/6J/129S4 mixed genetic background. Vaginal plug of the females was checked daily in the morning. Noon on the day when vaginal plug was found was considered embryonic day (E) 0.5. Genotyping was done by PCR on tail lysates following protocol described in the references.

Skeletal preparations

E18.5 embryos were dissected in PBS followed by removal of the skin and internal organs. After incubation in 95% ethanol overnight at room temperature, skeletons were stained with staining solution (0.005% alizarin red, 0.015% alcian blue and 5% glacial acetic acid in 70% ethanol) for 2 days at 37°C. The skeletons were then rinsed briefly in 95% ETOH at room temperature, and then cleared with 1% KOH overnight. Samples were then equilibrated in gradient washes of glycerol/KOH mixture until glycerol concentration reached 80%.

Histology and AP-AB staining

Timed embryos were harvested in ice-cold PBS. Embryos were decapitated and heads were fixed in 4% paraformaldehyde (PFA) in PBS for 18 – 24 hours at 4°C. Following dehydration with graded washes of ethanol, samples were embedded in paraffin and processed for 10μm frontal sections and subjected to standard Hematoxylin/Eosin staining or Alkaline Phosphatase and Alcian Blue (AP-AB) double staining. For AP-AB staining, sections were deparaffinized in Histo-clear followed by graded ethanol and incubated in 0.03% nitro-blue tetrazolium chloride (NBT) and 0.02% 5-bromo-4-chloro-3′-indolyphosphate p-toluidine salt (BCIP) to detect AP activity. Slides were then rinsed in water and dipped in 1% alcian blue 8GX (A5268, Sigma) in 0.1N HCl to label cartilage, and counterstained with 0.1% nuclear fast red solution.

In situ hybridization and immunohistochemistry

In situ hybridization was carried out as described previously (He and Soriano, 2013). *Pten* antisense RNA probes was generated using primers: 5-TTACAGTTGGGCCCCGTACA-3 and 5- TAAAACACCCACACAATGACAAGA-3. For immunohistochemistry, samples were sectioned at 10μm and subjected to standard protocols using primary antibodies to anti-phospho-Akt (1:25, Cell Signaling Technology 9271), anti-Neurofilament-L (1:100, Cell Signaling Technology 2837), HRP-conjugated secondary antibody (1:100, Cell Signaling Technology 7074), anti-Sp7(1:200, Abcam ab94744) and AP-conjugated secondary antibody (1:100, Novus Biologicals, NB7157).)

Quantitative PCR

Expression of *Runx2*, *Sp7* and *Osteocalcin* mRNA were analyzed by real-time quantitative RT-PCR. The premaxilla and adjacent medial nasal tissues were dissected from E13.5 embryos in ice cold PBS and total RNA was extracted using the RNeasy Mini Kit (Qiagen 74104). First strand cNDA was synthesized using 1μg of total RNA, oligo-dT primers and SuperScript III RT (Invitrogen 18080). Quantitative PCR was performed on Bio-Rad iCycler using SYBR super mix kit (Bio-Rad 170-8880). The following protocol was used: step 1: 95°C for 10 min; step 2: 95°C for 10 s; step 3: 55° for 30 s; repeat to step 2 39× (40 cycles in total). PCR products were run on agarose gel to confirm correct amplicon size. β-actin expression was used as an internal control. The primers are as follows: mouse Runx2, 5′-CCCAGCCACCTTTACCTACA-3′ and 5′-TATGGAGTGCTGCTGGTCTG-3′; mouse Sp7, 5′-AGTTCACCTGCCTGCTCTGT-3′ and 5′-GGAGCTGGAGACCTTCCTCT-3′; mouse osteocalcin, 5′-AAGCAGGAGGGCAATAAGGT-3′ and 5′-ACTTGCAGGGCAGAGAGAGA-3′; mouse β-actin, 5′-GCAAGTGCTTCTAGGCGGAC-3′ and 5′-AAGAAAGGGTGTAAAACGCAGC-3′.

Cell proliferation assay

For mice, BrdU was administered into pregnant female mice by intraperitoneal (I.P.) injection at 30 ug/g body weight. Embryos were dissected after 1 hour of injection, fixed in Carnoy's solution for 1 hour, dehydrated through graded ethanol washes, cleared in Histo-clear and embedded in paraffin. Frontal sections were cut at 10μm. Immunostaining for BrdU was performed using a Bromodeoxyuridine (BrdU) Labeling and Detection Kit (Roche, 11299964001). At least three embryos for each genotype and each stage were analyzed. BrdU labeled cells were counted in the pmx area in mutant and control samples. Data from three continuous sections of each embryo were collected for statistical analysis.

For cells, primary cells were incubated with 10 ug/ml BrdU for 30 minutes and were washed in PBS. The cells were then fixed in 4% PFA followed by incubation in 1N HCl for 10 minutes. Subsequently, the cells were blocked with 10% donkey serum for 1 hour, followed by incubation with anti-BrdU antibody (1:200, Novus Biologicals, NBP2-14890) for 1 hour and Alexa FluoR 448 donkey anti-rabbit IgG secondary antibody (Abcam, ab150073). DAPI was used for nuclei staining. BrdU labeled cells were counted in comparable areas in mutant and control samples. Data collected from at least three independent experiments were subject for statistical analysis using student's t-test. Statistical data are presented as mean ± SEM, and subjected to double tailed Student's t-tests.

Western blot

E13.5 embryos were dissected in ice-cold PBS. With the brain removed, the embryonic head was homogenized by sonication in ice-cold NP-40 buffer with proteinase inhibitors including protease inhibitor cocktail (Roche, 11836153001), 1 mM PMSF, 10 mM NaF, 1 mM Na_3VO_4 and 25 mM β-glycerophosphate. Tissue lysates were then centrifuged at 12000 rpm at 4°C. Supernatants were collected and protein concentrated was determined by BCA assay. Western blot was carried out using the primary antibodies from Cell Signaling Technology: Anti-β-actin (8457), anti-phospho-Akt (9271), and the secondary antibody from LI-COR Biosciences: IRDye 680RD (925-68071). An Odyssey CLx imaging system was used for result recording. ImageJ software was used to quantify the western blot result.

Acknowledgments

This work is supported by NIH/NIDCR grant R00DE024617 to F.H.

We thank YiPing Chen for the constructive comments. We are grateful to our laboratory colleagues for their comments and discussion on the manuscript. This work is supported by NIH/NIDCR grant R00DE024617 to F.H.

References

Arico S, Petiot A, Bauvy C, Dubbelhuis PF, Meijer AJ, Codogno P, Ogier-Denis E. The tumor suppressor PTEN positively regulates macroautophagy by inhibiting the phosphatidylinositol 3-kinase/protein kinase B pathway. J Biol Chem. 2001; 276:35243–35246. [PubMed: 11477064]

Chai Y, Jiang X, Ito Y, et al. Fate of the mammalian cranial neural crest during tooth and mandibular morphogenesis. Development. 2000; 127:1671–1679. [PubMed: 10725243]

Chai Y, Maxson RE Jr. Recent advances in craniofacial morphogenesis. Dev Dyn. 2006; 235:2353–2375. [PubMed: 16680722]

Cho KW, Cho SW, Lee JM, Lee MJ, Gang HS, Jung HS. Expression of phosphorylated forms of ERK, MEK, PTEN and PI3K in mouse oral development. Gene Expr Patterns. 2008; 8:284–290. [PubMed: 18203667]

Cordero DR, Brugmann S, Chu Y, Bajpai R, Jame M, Helms JA. Cranial neural crest cells on the move: their roles in craniofacial development. Am J Med Genet A. 2011; 155A:270–279. [PubMed: 21271641]

Di Cristofano A, Pesce B, Cordon-Cardo C, Pandolfi PP. Pten is essential for embryonic development and tumour suppression. Nat Genet. 1998; 19:348–355. [PubMed: 9697695]

Errafiy R, Aguado C, Ghislat G, Esteve JM, Gil A, Loutfi M, Knecht E. PTEN increases autophagy and inhibits the ubiquitin-proteasome pathway in glioma cells independently of its lipid phosphatase activity. PLoS ONE. 2013; 8:e83318. [PubMed: 24349488]

Fantauzzo KA, Soriano P. PI3K-mediated PDGFRalpha signaling regulates survival and proliferation in skeletal development through p53-dependent intracellular pathways. Genes Dev. 2014; 28:1005–1017. [PubMed: 24788519]

Fantauzzo KA, Soriano P. Receptor tyrosine kinase signaling: regulating neural crest development one phosphate at a time. Curr Top Dev Biol. 2015; 111:135–182. [PubMed: 25662260]

Ford-Hutchinson AF, Ali Z, Lines SE, Hallgrimsson B, Boyd SK, Jirik FR. Inactivation of Pten in osteo-chondroprogenitor cells leads to epiphyseal growth plate abnormalities and skeletal overgrowth. J Bone Miner Res. 2007; 22:1245–1259. [PubMed: 17456009]

Fraser MM, Bayazitov IT, Zakharenko SS, Baker SJ. Phosphatase and tensin homolog, deleted on chromosome 10 deficiency in brain causes defects in synaptic structure, transmission and plasticity, and myelination abnormalities. Neuroscience. 2008; 151:476–488. [PubMed: 18082964]

Groszer M, Erickson R, Scripture-Adams DD, Lesche R, Trumpp A, Zack JA, Kornblum HI, Liu X, Wu H. Negative regulation of neural stem/progenitor cell proliferation by the Pten tumor suppressor gene in vivo. Science. 2001; 294:2186–2189. [PubMed: 11691952]

Guntur AR, Reinhold MI, Cuellar J Jr, Naski MC. Conditional ablation of Pten in osteoprogenitors stimulates FGF signaling. Development. 2011; 138:1433–1444. [PubMed: 21385768]

He F, Soriano P. A critical role for PDGFRalpha signaling in medial nasal process development. PLoS Genet. 2013; 9:e1003851. [PubMed: 24086166]

Hsieh SC, Chen NT, Lo SH. Conditional loss of PTEN leads to skeletal abnormalities and lipoma formation. Mol Carcinog. 2009; 48:545–552. [PubMed: 18973188]

Jiang X, Rowitch DH, Soriano P, McMahon AP, Sucov HM. Fate of the mammalian cardiac neural crest. Development. 2000; 127:1607–1616. [PubMed: 10725237]

Kero D, Cigic L, Medvedec Mikic I, Galic T, Cubela M, Vukojevic K, Saraga-Babic M. Involvement of IGF-2, IGF-1R, IGF-2R and PTEN in development of human tooth germ - an immunohistochemical study. Organogenesis. 2016; 12:152–167. [PubMed: 27326759]

Klinghoffer RA, Hamilton TG, Hoch R, Soriano P. An Allelic Series at the PDGFalphaR Locus Indicates Unequal Contributions of Distinct Signaling Pathways During Development. Dev Cell. 2002; 2:103–113. [PubMed: 11782318]

Knecht AK, Bronner-Fraser M. Induction of the neural crest: a multigene process. Nat Rev Genet. 2002; 3:453–461. [PubMed: 12042772]

Lehtinen MK, Zappaterra MW, Chen X, Yang YJ, Hill AD, Lun M, Maynard T, Gonzalez D, Kim S, Ye P, D'Ercole AJ, Wong ET, LaMantia AS, Walsh CA. The cerebrospinal fluid provides a proliferative niche for neural progenitor cells. Neuron. 2011; 69:893–905. [PubMed: 21382550]

Lewis AE, Vasudevan HN, O'Neill AK, Soriano P, Bush JO. The widely used Wnt1-Cre transgene causes developmental phenotypes by ectopic activation of Wnt signaling. Dev Biol. 2013; 379:229–234. [PubMed: 23648512]

Li DM, Sun H. TEP1, encoded by a candidate tumor suppressor locus, is a novel protein tyrosine phosphatase regulated by transforming growth factor beta. Cancer Res. 1997; 57:2124–2129. [PubMed: 9187108]

Marino S, Krimpenfort P, Leung C, van der Korput HA, Trapman J, Camenisch I, Berns A, Brandner S. PTEN is essential for cell migration but not for fate determination and tumourigenesis in the cerebellum. Development. 2002; 129:3513–3522. [PubMed: 12091320]

Salmena L, Carracedo A, Pandolfi PP. Tenets of PTEN tumor suppression. Cell. 2008; 133:403–414. [PubMed: 18455982]

Sauka-Spengler T, Bronner-Fraser M. A gene regulatory network orchestrates neural crest formation. Nat Rev Mol Cell Biol. 2008; 9:557–568. [PubMed: 18523435]

Selleck MA, Bronner-Fraser M. Origins of the avian neural crest: the role of neural plate-epidermal interactions. Development. 1995; 121:525–538. [PubMed: 7768190]

Steck PA, Pershouse MA, Jasser SA, Yung WK, Lin H, Ligon AH, Langford LA, Baumgard ML, Hattier T, Davis T, Frye C, Hu R, Swedlund B, Teng DH, Tavtigian SV. Identification of a candidate tumour suppressor gene, MMAC1, at chromosome 10q23.3 that is mutated in multiple advanced cancers. Nat Genet. 1997; 15:356–362. [PubMed: 9090379]

Steelman LS, Bertrand FE, McCubrey JA. The complexity of PTEN: mutation, marker and potential target for therapeutic intervention. Expert Opin Ther Targets. 2004; 8:537–550. [PubMed: 15584861]

Vasudevan HN, Mazot P, He F, Soriano P. Receptor tyrosine kinases modulate distinct transcriptional programs by differential usage of intracellular pathways. Elife. 2015:4.

Veleva-Rotse BO, Barnes AP. Brain patterning perturbations following PTEN loss. Front Mol Neurosci. 2014; 7:35. [PubMed: 24860420]

Yang G, Sun Q, Teng Y, Li F, Weng T, Yang X. PTEN deficiency causes dyschondroplasia in mice by enhanced hypoxia-inducible factor 1alpha signaling and endoplasmic reticulum stress. Development. 2008; 135:3587–3597. [PubMed: 18832389]

Yoshida T, Vivatbutsiri P, Morriss-Kay G, Saga Y, Iseki S. Cell lineage in mammalian craniofacial mesenchyme. Mech Dev. 2008; 125:797–808. [PubMed: 18617001]

Yue Q, Groszer M, Gil JS, Berk AJ, Messing A, Wu H, Liu X. PTEN deletion in Bergmann glia leads to premature differentiation and affects laminar organization. Development. 2005; 132:3281–3291. [PubMed: 15944184]

Zhang M, Xuan S, Bouxsein ML, von Stechow D, Akeno N, Faugere MC, Malluche H, Zhao G, Rosen CJ, Efstratiadis A, Clemens TL. Osteoblast-specific knockout of the insulin-like growth factor (IGF) receptor gene reveals an essential role of IGF signaling in bone matrix mineralization. J Biol Chem. 2002; 277:44005–44012. [PubMed: 12215457]

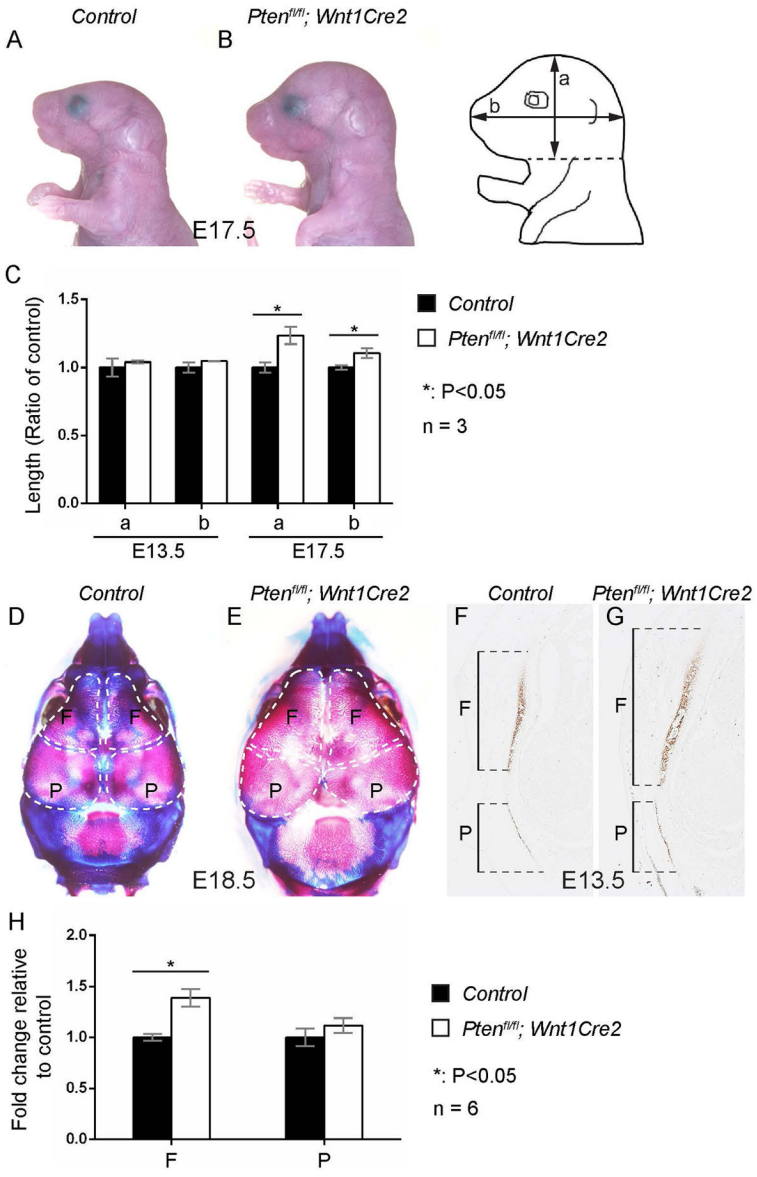

Fig 1. Inactivating *Pten* in NCCs leads to an enlarged skull

(A, B) Lateral view of the littermate control (A) and *Pten*$^{fl/fl}$*; Wnt1Cre2* (B) at E17.5. (C) Morphometric quantification and statistical analysis of the control and *Pten*$^{fl/fl}$*; Wnt1Cre2* embryos along the dorsal-ventral axis (a) and anterior-posterior axis (b) at E13.5 and E17.5 (n=3). (D, E) Dorsal view of skeletal preparations of littermate control (D) and *Pten*$^{fl/fl}$*; Wnt1Cre2* (E) at E18.5. (F, G) Immunostaining with anti-Sp7 antibody on transverse sections of the control and *Pten*$^{fl/fl}$*; Wnt1Cre2* embryos at E13.5. (H) Quantification and statistical analysis of the frontal bone and parietal bone length of F and G. F, frontal bone. P, parietal bone.

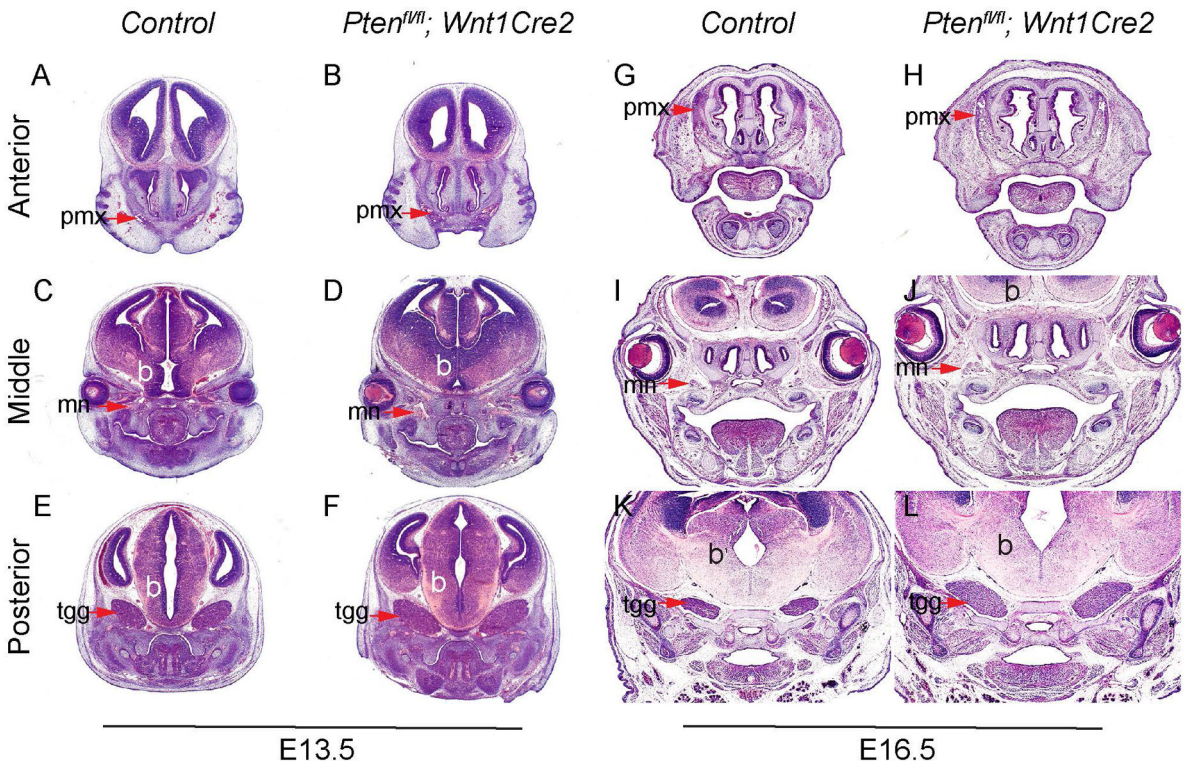

Fig 2. *Pten*$^{fl/fl}$; *Wnt1Cre2* embryos exhibit overgrowth of craniofacial tissues

H&E staining on frontal sections of littermate control and *Pten*$^{fl/fl}$; *Wnt1Cre2* at E13.5 (A–F) and at E16.5 (G–L). Arrows point to pmx in A, B, G and H, to mn in C, D, I and J, and to tgg in E, F, K and L. b, brain; mn, maxillary nerve; pmx, premaxilla; tgg, trigeminal ganglion.

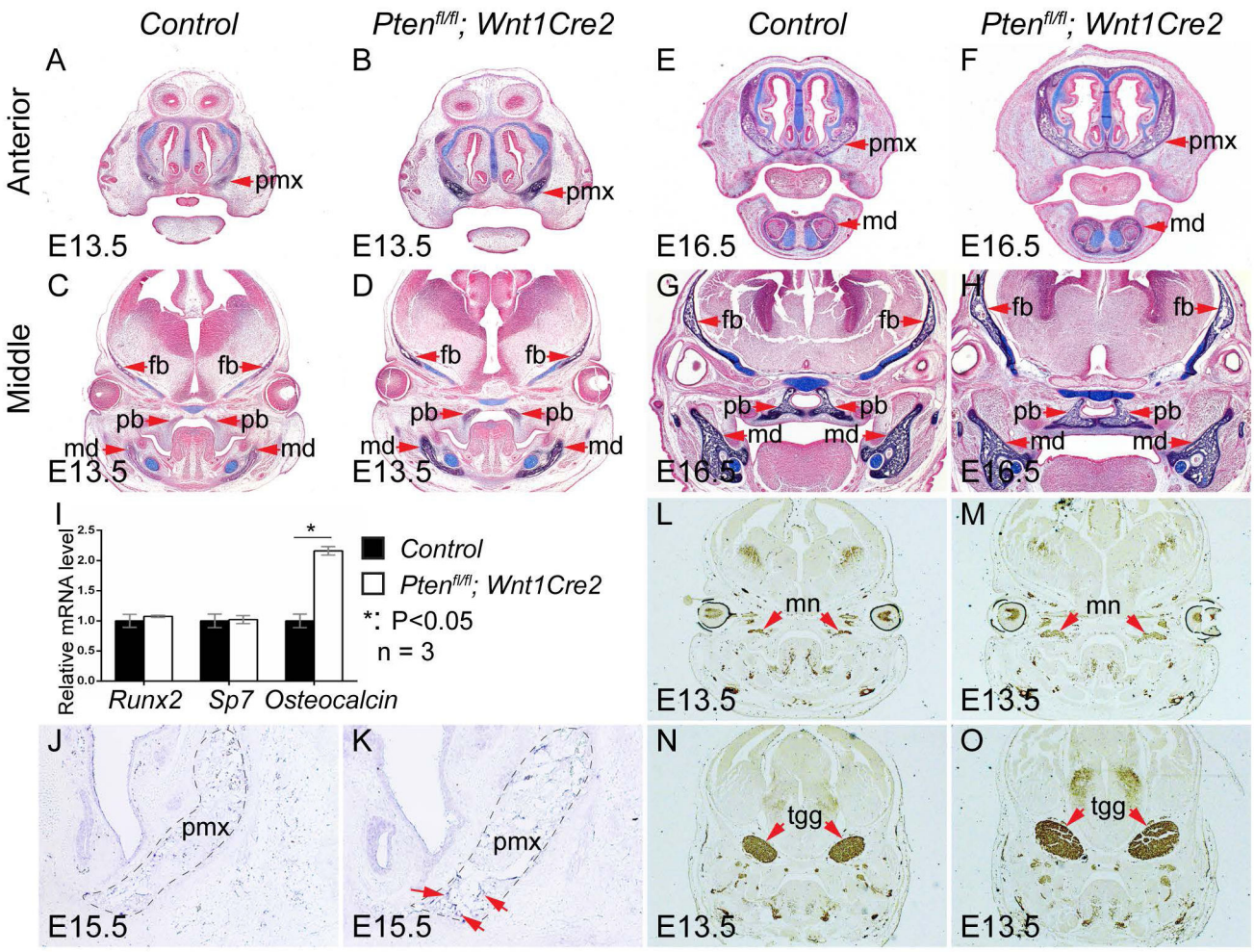

Fig 3. *Pten* deficiency causes enhanced osteoblast differentiation and neurogenesis

(A–H) AP-AB staining on frontal sections of littermate control and *Pten*$^{fl/fl}$; *Wnt1Cre2* embryos at E13.5 (A–D) and at E16.5 (E–H). Sections were counterstained with nuclear fast red. (I) Quantification result of osteogenesis markers expression of the control and *Pten*$^{fl/fl}$; *Wnt1Cre2* mRNA samples prepared from E13.5 embryos (n=3). (J, K) *In situ* hybridization with *Osteocalcin* antisense probe on the frontal sections of the control (J) and *Pten*$^{fl/fl}$; *Wnt1Cre2* (K) embryos at E15.5. (L–O) Immunostaining with anti-Neurofilament-L antibody on frontal sections of littermate control (L, N) and *Pten*$^{fl/fl}$; *Wnt1Cre2* (M, O) embryos at E13.5. fb, frontal bone; md, mandible; mn, maxillary nerve; pb, palatine bone; pmx, premaxilla; and tgg, trigeminal ganglion.

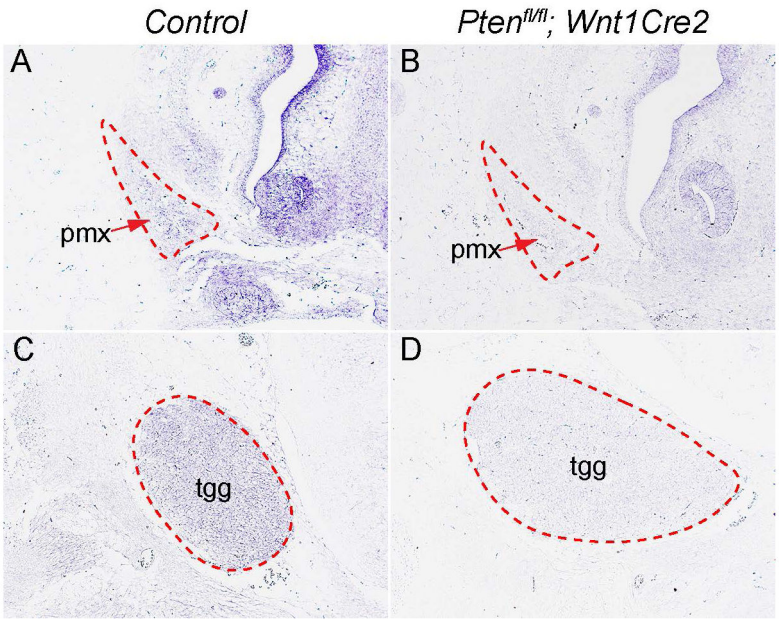

Fig 4. Expression pattern of *Pten* mRNA in developing craniofacial structures

(A–D) *In situ* hybridization using *Pten* antisense probe on frontal sections of wild type (A, C) and of *Pten*$^{fl/fl}$; *Wnt1Cre2* (B, D) embryos at E13.5. pmx, premaxilla; tgg, trigeminal ganglion.

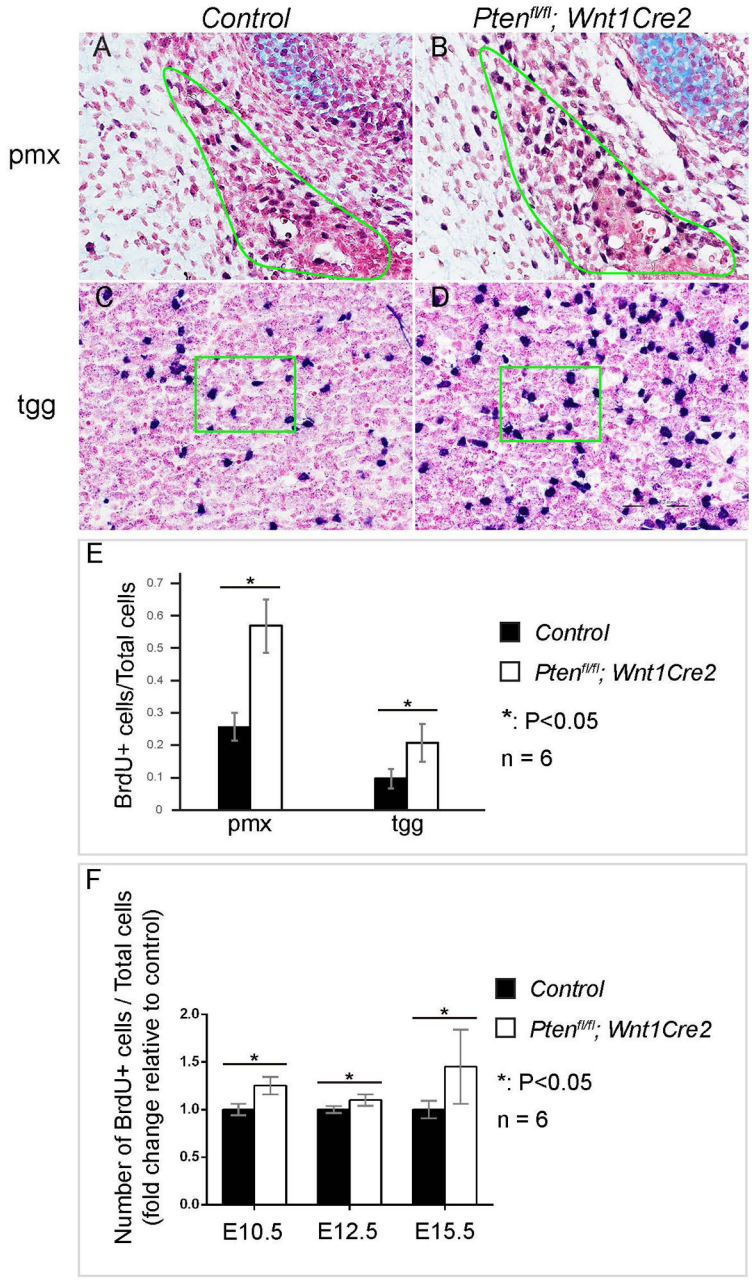

Fig 5. *Pten* is essential to regulate proliferation of osteoprogenitors and tgg cells

(A–D) BrdU labeling on frontal sections of littermate control (A, C) and *Pten*$^{fl/fl}$; *Wnt1Cre2* (B, D) at E13.5, with a focus on pmx (A, B) and tgg (C, D). Slides were counterstained with nuclear fast red to facilitate quantification. (E) Quantification result and statistical analysis of percentage of BrdU+ cells in control and *Pten*$^{fl/fl}$; *Wnt1Cre2* tissues. (F) Quantification and statistical analysis of the percentage of BrdU+ cells in *Pten*$^{fl/fl}$; *Wnt1Cre2* and littermate control pmx at E10.5, E12.5 and E15.5. The result is presented as fold change relative to the control. pmx, premaxilla; tgg, trigeminal ganglion.

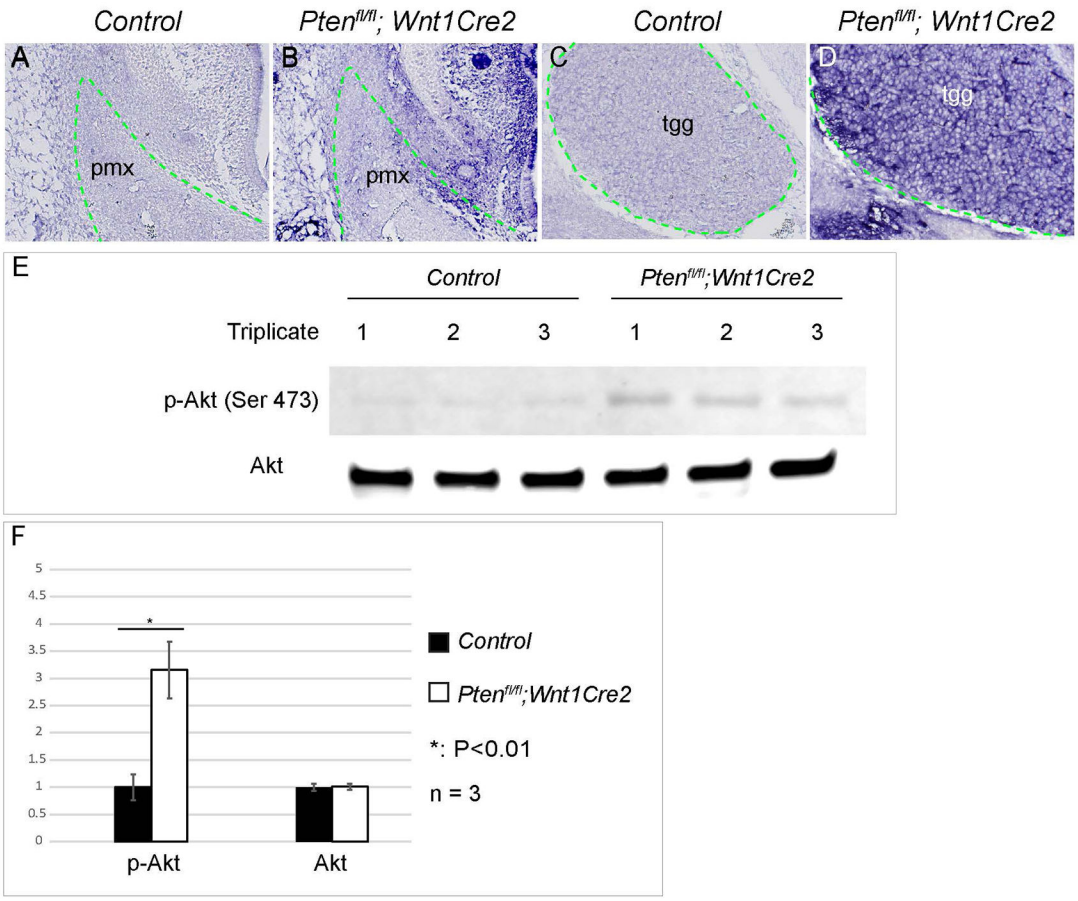

Fig 6. *Pten* deficiency increases PI3K/AKT signaling activity in neural crest cells

(A–D) Immunostaining with anti phospho-AKT antibody on frontal sections of littermate control embryos (A, C) and *Pten*$^{fl/fl}$*; Wnt1Cre2* (B, D) at E13.5. (E) Western blot using anti phospho-AKT antibody (p-Akt Ser473) and craniofacial lysates from littermate control and *Pten*$^{fl/fl}$*; Wnt1Cre2* embryos at E13.5. (F) Quantification result and statistical analysis of western blot data on E. pmx, premaxilla; tgg, trigeminal ganglion.

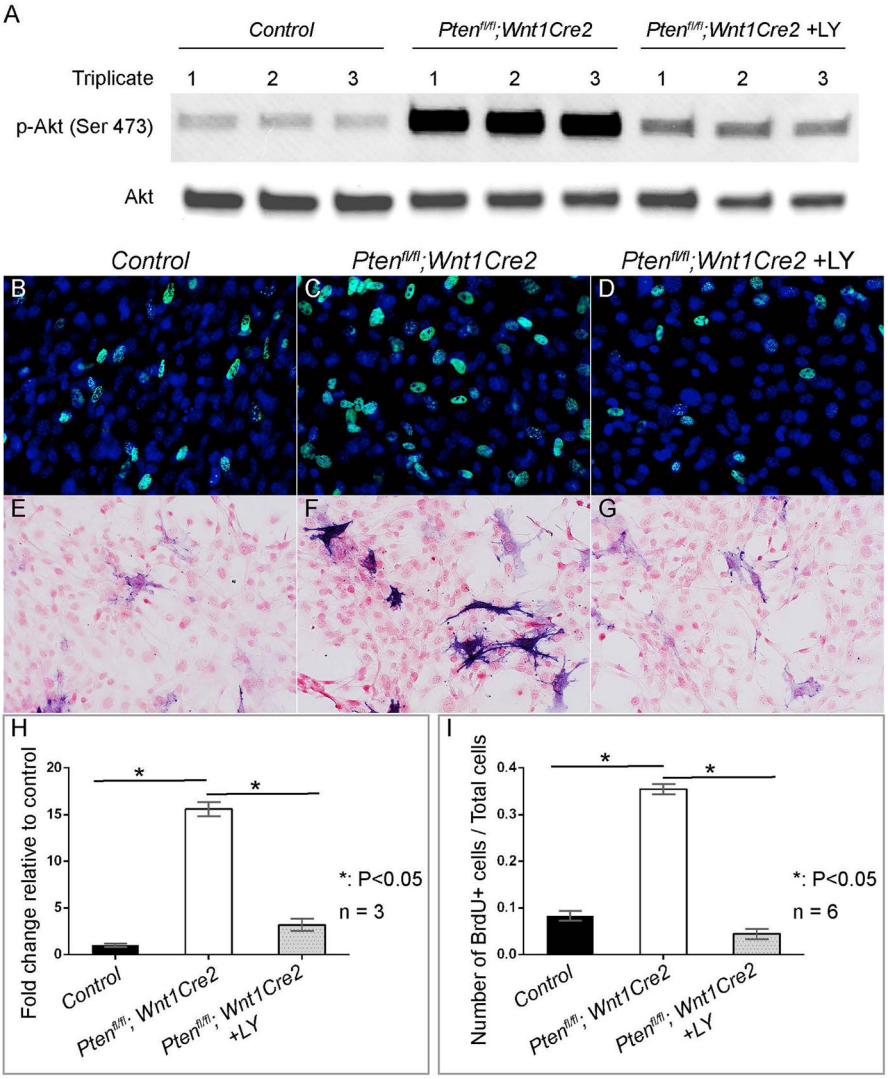

Fig 7. Inhibiting PI3K/AKT signaling rescues *Pten* mutant neural crest cells phenotype *in vitro*

(A) Western blot of phospho-AKT and total AKT in primary pmx cells prepared from littermate control and *Pten*$^{fl/fl}$*; Wnt1Cre2* embryos at E13.5. (B–D) BrdU labeling of primary pmx cells of littermate control (B), *Pten*$^{fl/fl}$*; Wnt1Cre2* (C) and *Pten*$^{fl/fl}$*; Wnt1Cre2* treated with 10uM LY for 30 minutes (D). BrdU+ cells are labeled with green fluorescence and total nuclei are stained with DAPI (blue). (E–G) AP staining of primary E13.5 pmx cells of littermate control (E), *Pten*$^{fl/fl}$*; Wnt1Cre2* (F) and *Pten*$^{fl/fl}$*; Wnt1Cre2* treated with 10uM LY for 8 hours (G). AP positive cells are blue and nuclei are counterstained with nuclear fast red. (H) Quantification and statistic analysis of western blot result of (A). (I) Quantification and statistic analysis of BrdU labeling results of (B–D).

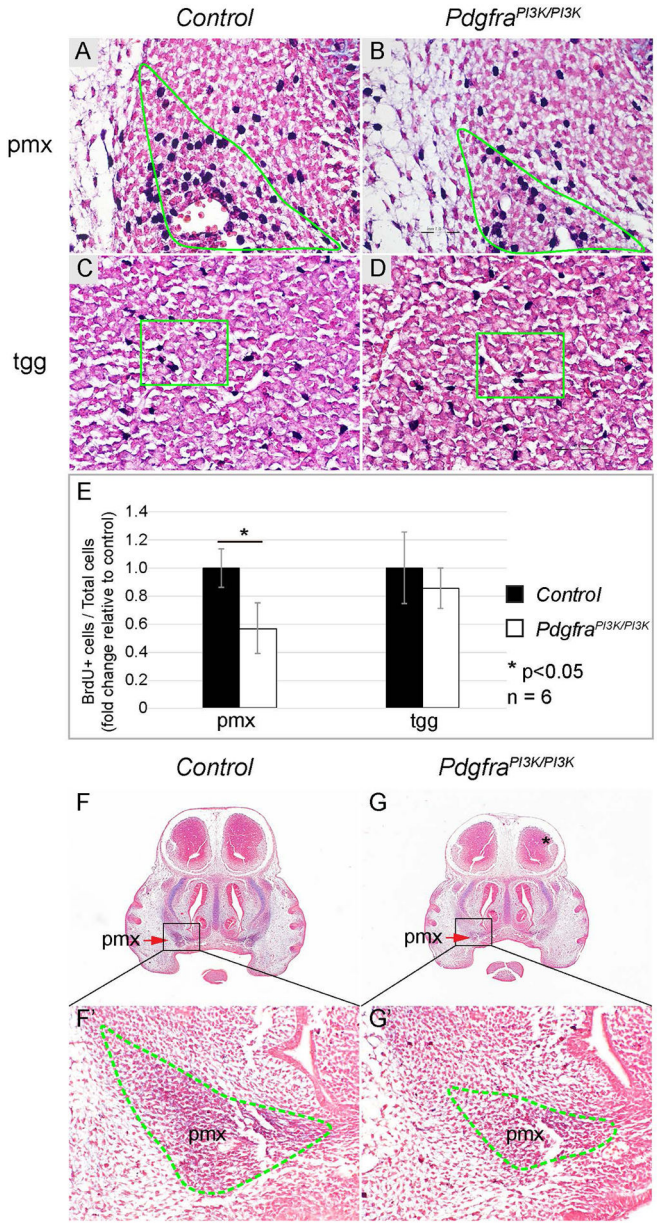

Fig 8. Attenuation of PI3K/AKT signaling affects NCCs proliferation and differentiation during craniofacial development

(A–D) BrdU labeling on frontal sections of littermate control (A, C) and *Pdgfra*$^{PI3K/PI3K}$ (B, D) embryos at E13.5, with a focus on the pmx (A, B) and tgg (C, D). Slides were counterstained with nuclear fast red to facilitate quantification. (E) Quantification and statistical analysis of percentile of BrdU+ cells in the control and *Pdgfra*$^{PI3K/PI3K}$ tissues. The result is presented as fold change relative to the control. (F, G) AP-AB staining on frontal sections of littermate control (F) and *Pdgfra*$^{PI3K/PI3K}$ (G) embryos at E13.5. (F′, G′) Magnification of defined area in F and G. pmx, premaxilla; tgg, trigeminal ganglion.